et al. The density of triplet excitons n is described by the equation

$$dn/dt = \alpha I - \beta n - \gamma n^2,$$

where αI represents the generation of excitons by the laser light, β is the reciprocal lifetime of the triplet exciton, and γ is the bimolecular interaction rate constant. From our data we find with an uncertainty of 50% the following values:

$$\alpha = 8.6\times10^{-6}\ \text{cm}^{-1},$$

$$\beta = 58\ \text{sec}^{-1},$$

$$\gamma = 5.5\times10^{-11}\ \text{cm}^3\ \text{sec}^{-1}.$$

Measurements of α and δ as a function of integrated laser power showed these quantities to be independent of the incident laser power up to approximately 500 kW cm^{-2}.[7] This would indicate that the creation of excitons is a first-order process, whereas the decay is via bimolecular recombination.

The Raman-shifted ruby line from nitrobenzene at 7670 Å[8] was used to determine the wavelength dependence of both processes. The power at 7670 Å was 500 kW. It was found that to within 50%, δ was independent of λ at 6943 Å and 7670 Å, and that

$$\alpha(\lambda = 6943\ \text{Å}) = 5.1\alpha(\lambda = 7670\ \text{Å}).$$

This further suggests that the generation of triplet excitons is a resonant process.

The experiments performed by Peticolas et al., Kepler et al., and the authors lead one to the following conclusions:

(1) The ruby laser can excite 2-photon processes and triplet excitons in the anthracene crystal leading to normal and delayed fluorescence, respectively.

(2) The ratio of the number of blue photons emitted by normal and by delayed fluorescence is proportional to the number of photons per square centimeter per second of the laser and independent of the total number of photons in each pulse. We believe this is the origin for the different conclusions reached in references 3 and 4.

(3) As expected on the basis of the crystal symmetry, anthracene is a very inefficient generator of optical second harmonics.

The authors would like to thank J. E. Drumheller for his help during the initial stages of the investigation.

[1]R. W. Hellwarth, Advances in Quantum Electronics, edited by J. Singer (Columbia University Press, New York, 1961), 2nd ed., pp. 334-341.

[2]F. J. McClung and R. W. Hellwarth, Bull. Am. Phys. Soc. 6, 414 (1961); J. Appl. Phys. 33, 838 (1962).

[3]W. L. Peticolas, J. P. Goldsborough, and K. E. Rieckhoff, Phys. Rev. Letters 10, 43 (1963); W. L. Peticolas and K. E. Rieckhoff, J. Chem. Phys. 39, 1347 (1963).

[4]R. G. Kepler, J. C. Caris, P. Avakian, and E. Abramson, Phys. Rev. Letters 10, 400 (1963).

[5]J. B. Birks, T. A. King, and I. H. Munro, Proc. Phys. Soc. (London) 80, 355 (1962).

[6]P. A. Franken, A. E. Hill, C. W. Peters, and G. Weinreich, Phys. Rev. Letters 7, 118 (1961).

[7]The interesting increase in α and associated decrease in δ at the higher intensities is presently being studied.

[8]Gisela Eckhardt, R. W. Hellwarth, F. J. McClung, S. E. Schwarz, and D. Weiner, Phys. Rev. Letters 9, 455 (1962).

INFRARED QUANTUM COUNTER ACTION IN Pr-DOPED FLUORIDE LATTICES

M. R. Brown
Ministry of Aviation, Signals Research and Development Establishment, Christchurch, Hampshire, England

and

W. A. Shand*
Department of Natural Philosophy, University of Aberdeen, Aberdeen, Scotland

(Received 20 September 1963)

The principle of the solid-state infrared quantum counter as proposed by Bloembergen,[1] that is, the excitation of fluorescence radiation by the simultaneous absorption of two photons, was demonstrated by Porter[2] using Pr^{3+} doped 1% in $LaCl_3$ at liquid helium temperature. This Letter reports infrared quantum counter action in Pr^{3+} doped 0.5% in LaF_3, SrF_2, CaF_2, and 2.5% in BaF_2 at both room and liquid nitrogen temperatures. The results show that the action has application both in spectroscopic measurements and as a narrow-band infrared detector sensitive to more than one infrared frequency.

The fluoride single crystals used in these ex-

periments were grown by the Stockbarger technique. They were mounted in a copper block in a metal Dewar provided with windows for optical access. The pumping sources were a ME/D mercury lamp and an A1/9 projection lamp, both being fitted with suitable filters to prevent the excitation of the fluorescence by direct absorption from the ground state. A Leiss double monochromator was used to separate the fluorescent output from the scattered pump radiation.

The three schemes identified are shown in Fig. 1. The energies given are the averages for each of the multiplets and are only approximate, for there are shifts between the various host lattices. The fluorescent output in each case is at 485 mμ. This was selected for three reasons; it was the strongest fluorescence, it fell in the region of the maximum sensitivity of the EMI-9558 photomultiplier, and it is at a shorter wavelength than any of the visible pumps used.

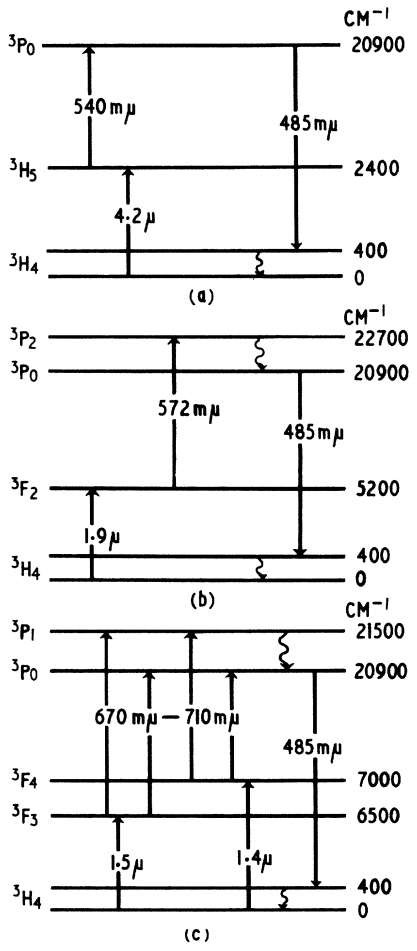

FIG. 1. The three infrared quantum counter schemes. Only the relevant energy levels of the Pr^{3+} ion are shown.

It is convenient to discuss the results for the four doped fluoride lattices by considering the schemes in turn:

Scheme 1 [Fig. 1(a)].—At room temperature the $^3H_5$ multiplet is populated thermally. With the visible pump on alone, action occurs in LaF_3 and SrF_2 lattices. The signal-to-noise ratio in these two cases was 15:1. This action disappears at liquid nitrogen temperatures.

Scheme 2 [Fig. 1(b)].—This scheme occurs in the LaF_3, SrF_2, and CaF_2 lattices at both room and liquid nitrogen temperatures but only at liquid nitrogen temperature for the BaF_2 crystal. The signal-to-noise ratio for the fluorescent output at liquid nitrogen temperature was 50:1, 30:1, 10:1, and 2:1 for the LaF_3, SrF_2, CaF_2, and BaF_2 lattices, respectively.

The insertion of a filter to cut out the 1.9-μ infrared radiation does not kill this scheme completely in the LaF_3, SrF_2, and CaF_2 crystals because there is relaxation down into the $^3F_2$ multiplet from the $^3F_3$ and $^3F_4$ multiplets above [shown in Fig. 1(c)]. This relaxation process can contribute as much as 10% to the scheme's fluorescent output. There has been no definite sign of the corresponding relaxation from the $^3F_2$ multiplet down to the $^3H_6$ multiplet.

It has not been possible to do similar measurements on the BaF_2 crystal because of the poor output signal-to-noise ratio.

Scheme 3 [Fig. 1(c)].—This scheme only occurs in the LaF_3 crystal and then only at liquid nitrogen temperature. It has not been possible to narrow down the transitions involved to less than those shown in Fig. 1(c). However, the measurements point towards the $^3F_4$ multiplet as playing a dominant role.

The development of narrow-band infrared detectors based on the quantum counter principle is now a very attractive proposition, for the existence of these three schemes in one crystal means that the detector would be sensitive to three infrared frequencies.

These results also show that the action has a possible application as a technique (a) for measuring relaxation rates between the low-lying levels and (b) for locating levels which may, in some materials, be inside the host lattice absorption band.

(a) In Scheme 2, as an example, there are two relaxation processes; the $^3F_3$ and $^3F_4$ multiplets to $^3F_2$ multiplet relaxation and the $^3F_2$ multiplet to $^3H_6$ multiplet relaxation. The components in the fluorescent output that are influenced by these

processes may be seen independently by the use of infrared filters. The method is essentially an extension of the phase method of measuring radiative lifetimes. To measure the relaxation rates for the first process, the infrared and optical pumps should be chopped at the same frequency and then any phase shift in the fluorescent output will be a measure of the relaxation rate. For the second process the pumps should be chopped so that the beat frequency is constant and then a change in the beat frequency amplitude will occur when the infrared chopping frequency is approximately the relaxation rate. This assumes the relaxation times are less than the fluorescent lifetime.

(b) As can be seen from Scheme 1, provided the levels are thermally populated, then absorption transitions from these levels can be detected even though direct absorption to these levels is masked by the host lattice absorption.

We wish to thank Professor R. V. Jones for extending to us the facilities of his department and to Dr. D. A. Jones for assistance in growing the crystals.

*On detached duty at Signals Research and Development Establishment, Christchurch, Hampshire, England.

[1]N. Bloembergen, Phys. Rev. Letters 2, 84 (1959).
[2]J. F. Porter, Phys. Rev. Letters 7, 414 (1961).

QUANTUM EFFECTS IN THE INFRARED REFLECTIVITY OF BISMUTH

L. C. Hebel and P. A. Wolff
Bell Telephone Laboratories, Murray Hill, New Jersey
(Received 9 September 1963)

Recent experiments[1] have shown unequivocally that the energy-momentum relation for electrons in Bi is nonparabolic. In addition, the small Fermi energy, E_F, and light cyclotron masses in this material make it possible, with modest magnetic fields, to achieve Landau-level spacings which are comparable to E_F. Such a situation is ideally suited to the observation of quantum effects in cyclotron resonance. We report here on infrared reflectivity measurements which show pronounced effects of this type. These are of particular interest since they give information about the band structure away from the point $k_z = 0$. The data are analyzed in terms of Lax's[2] two-band model for Bi and are consistent with it.

In the two-band model, the energy of the nth Landau level in a conduction band of Bi is given by the expression

$$E_n = \{(\tfrac{1}{2}E_G)^2 + E_G[h^2k_z^2/2m_z + nh\omega_c]\}^{1/2} - (\tfrac{1}{2}E_G), \quad (1)$$

in which E_G is the band gap, ω_c the cyclotron frequency, and k_z the electron momentum in the magnetic field direction as measured from the band minimum. Figure 1 shows the corresponding variation with k_z of the three lowest Landau level energies. The magnetic field, B, has been chosen in such a way that the $n = 2$ Landau subband lies entirely above the Fermi surface, whereas the $n = 1$ subband cuts it. Such were the circumstances under which the most pronounced quantum effects were observed. For B parallel to the binary axis in Bi, they are

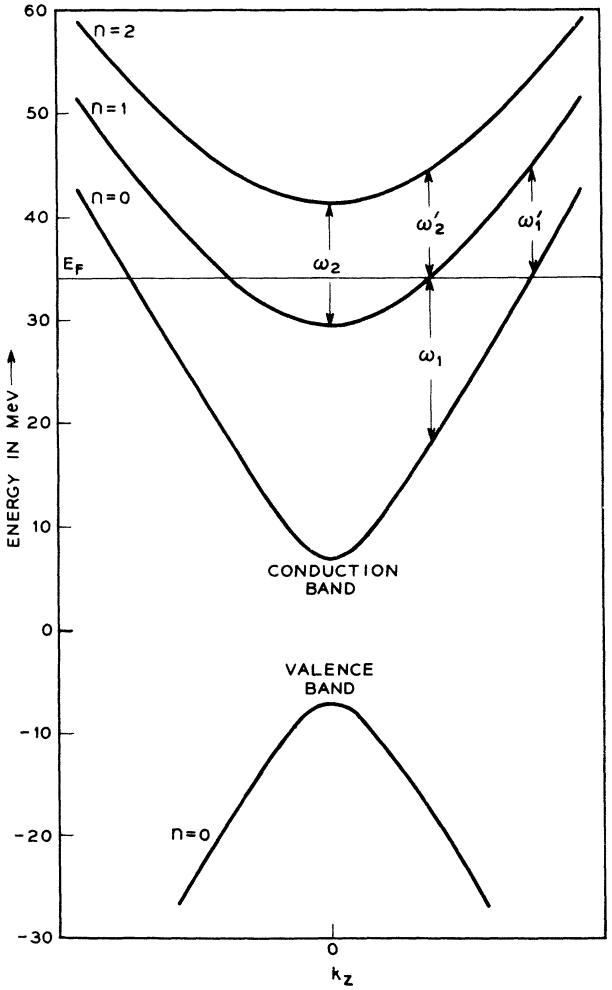

FIG. 1. Plot of Landau-level energy versus k_z.